J Mater Sci (2010) 45:354–362
DOI 10.1007/s10853-009-3943-4

Thermal stability and strength of Mo/Pt multilayered films

A. Bellou · L. Scudiero · D. F. Bahr

Received: 29 July 2009 / Accepted: 2 October 2009 / Published online: 15 October 2009

Abstract The strength of Mo/Pt multilayers of varying thicknesses has been investigated using nanoindentation. Metallic composites with individual layer thicknesses ranging from 100 to 20 nm were fabricated. Of specific interest in this study was the strength of the nanocomposites after annealing in air at relatively high temperatures (475 °C) since potential applications involve high temperature and oxidizing environments. Annealing causes significant losses in strength, with the highest losses corresponding to the structures with the thinner Pt layers. Annealing caused grain coarsening as well as loss of the continuous interface between the individual layers when the Pt thickness was less than 35 nm. Oxidation of the Mo layers occurred during annealing, causing an increase in the thickness of the Mo containing layers. The oxidation of Mo occurs in a uniform manner which results in an increase of the total film thickness while the layered structure is maintained. Deconvolution of the Mo 3d spectrum from X-ray Photoelectron Spectroscopy revealed several oxide species, and no Pt–Mo intermetallics were detected. The changes in microstructure are related to the changes in mechanical properties. Films with thinner layer thicknesses were stronger prior to annealing; however, they showed larger losses in strength after the thermal treatment. Structures with thicker Pt layers should be used when the multilayers are exposed to elevated temperatures.

A. Bellou · D. F. Bahr (✉)
School of Mechanical and Materials Engineering, Washington State University, P.O. Box 642920, Pullman, WA 99164-2920, USA
e-mail: dbahr@wsu.edu

L. Scudiero
Department of Chemistry, Washington State University, Pullman, WA, USA

Introduction

Composite structures that consist of two alternating thin metal layers have attracted a considerable amount of interest due to their improved mechanical properties when compared to those of their individual constituents. The layering of a soft metal with a harder one yields higher strength values than would be expected by a simple rule of mixtures, with the strength increasing as the thickness of the layers decreases [1–4]. The interface between the two metals can be either coherent or incoherent. In the first case (for example Cu–Ni) the strengthening is due in part to the elastic mismatch between the two films. In the second case (for example Cu–Nb) the interface acts as a substantial barrier to dislocation motion. For these multicomponent systems both layer thickness and interface type determine the overall mechanical behavior, with incoherent interfaces generally yielding at higher strength values than the coherent case.

The mechanical properties of multilayered structures have been primarily investigated at room temperature. However, some potential applications involve high temperature or oxidizing environments and thermal excursions, which make the long-term stability an important issue. The composite with improved mechanical properties must maintain its strength at high temperatures in order to be a viable candidate for these conditions. Studies of nanolayered systems have shown that stability at high temperatures can be a concern [5, 6]. For instance, annealing Ta/Cu films at temperatures ranging from 400 to 800 °C showed complete disintegration of the layered structure at 800 °C [5] with a final microstructure of equiaxed Cu and Ta grains. Experiments on the thermal stability of Cu/Nb films with layer thicknesses of 15, 35, and 75 nm at temperatures up to 800 °C for times reaching 60 h, showed that the

nanostructures with thicknesses of 35 and 75 nm were stabilized by the alignment of triple point junctions in a zigzag pattern [6]. This alignment seemed to protect the structure from layer pinch off and subsequent spheroidization. Hence the composites maintained most of their strength with the 75 nm thickness being stable even after 60 h at 700 °C. Although realignment of the grain boundaries did occur in 15 nm thick layers it did not effectively stabilize the structure. In the thinnest films at 700 °C even short annealing times (30 min) caused the loss of the layered structure which resulted in a significant decrease of the film hardness. This demonstrates that maintaining the layered structure at high temperatures is crucial in retaining the high strength of the nanocomposite.

While many multilayer studies have focused on Cu as the FCC metal [7–9], it is not the only FCC metal of interest in thin film applications. Pt is used in applications as an electrode for high temperature oxidizing conditions. For instance, Pt electrodes are commonly used for fabricating piezoelectric $Pb(Zr_xTi_{1-x})O_3$ films [10]. Piezoelectric films in membrane form can be used as MEMS acoustic transducers, and they exhibit enhanced performance when operated at high strains [11]. Silicon (Si) is commonly added as a support layer which helps the membrane withstand high pressures. At high strains the support layer does not add to the efficiency of the device so there is interest in removing it from the structure. In this case the bottom electrode could act both as the electrical component and the support layer of the piezoelectric actuator. However, Pt develops high residual tensile stresses after deposition and subsequent MEMS processing, and is generally not a suitable free standing film for membranes with a thickness on the order of 1 μm and lateral dimensions on the order of millimeters. Layering of Pt with another metal could improve the mechanical properties of the film and allow fabrication of free standing membranes.

In the current study molybdenum (Mo) was chosen as the second metal to be used with Pt in multilayered structures. Mo forms an incoherent interface with the Pt layer, and thus should result in high strength films. Additionally, Mo has some solid solubility in Pt and does form intermetallic phases with Pt, and as such is representative of many of the bcc metals with Pt. Mo/Pt multilayers with a number of different thickness combinations were sputtered and their strength was evaluated using nanoindentation. In each case the strength of the composite was higher than that of the Pt film alone making these nanolayered structures attractive for MEMS applications. Since piezoelectric MEMS processing often involves high temperature annealing in air [10] the thermal stability and oxidation of these composites is an important issue in addition to problems such as the pinching off of layers and grain coarsening already reported for other multilayered systems [5, 6].

In order to study the thermal stability of the Mo/Pt system and investigate the changes in the strength for films with different bilayer periods all structures were annealed at 475 °C for 1 h. The strength of the composites was determined using nanoindentation and the resulting microstructures were studied by Scanning Electron Microscopy (SEM). Bulk and surface chemical compositions were investigated by X-ray Diffraction (XRD) and X-ray Photoelectron Spectroscopy (XPS). Chemical bonding information was obtained by XPS. The use of these complementary techniques allowed a correlation between the observed microstructure, chemical properties, and the measured hardness of the annealed samples.

Experimental details

The nanolayered films used in this study were deposited by sequential DC magnetron sputtering at nominally room temperature. Films with 4, 10, and 20 layers were sputtered on thermally oxidized Si wafers with a SiO_2 layer approximately 120 nm thick, and the wafers were rotated over the sputtering guns to improve uniformity of the films. The Mo layer was always the first layer in the sequence directly sputtered on the oxide, with Pt being the last layer. The thicknesses of the nanolayered structures used in this study are shown in Table 1. The background pressure in the chamber prior to sputtering was 1×10^{-6} Torr. All Mo layers were sputtered at a regulated power of 200 W and an

Table 1 Specimens used in this study

Sample #	Nominal layer thickness [Mo (nm)/Pt (nm)]	Measured layer thickness [Mo (nm)/Pt (nm)]	Total film thickness (nm)
1 (20 layers)	20/20	18/21	430
2 (20 layers)	25/30	25/29	590
3 (10 layers)	60/35	61/35	503
4 (4 layers)	35/100	33/94	252
5 (4 layers)	55/100	55/107	336
6 (4 layers)	100/100	93/102	391

Both nominal and actual layer thicknesses are reported

Ar pressure of 3.8 mTorr while the Pt layers were sputtered at a regulated power of 60 W and an Ar pressure of 11 mTorr. The deposition rate for each metal was kept constant for all different composites and different layer thicknesses were obtained by accordingly varying the deposition time. In addition to the Mo/Pt multilayers that were deposited on Si wafers, films with the same bilayer period as samples 2 and 6 were also sputtered on glass substrates. The use of glass substrates allowed the acquisition of X-ray diffraction patterns from the films without the contribution of Si to the pattern. A Siemens D-500 X-ray powder diffractometer with a Cu X-ray tube was used to collect the diffraction data.

Films with the same bilayer period as samples 2 and 6 were also sputtered on Si/SiO_2 windows which were fabricated using standard photolithography techniques. The Si/SiO_2 backing substrate had a thickness of approximately 2.5 μm. These membranes were used to evaluate the residual stress in the as-deposited and annealed case using the bulge testing technique [12, 13]. The presence of compressive residual stresses in the as-deposited films caused sample 2 to buckle after deposition, so only results for the 100 nm/100 nm Mo/Pt film, as measured before and after annealing, are reported.

The thermal annealing of the various films was done in a Lindberg 1800 °C box furnace in air. The samples were heated at a rate of 8 °C/min to 475 °C and held at temperature for 1 h. The samples were then furnace cooled to room temperature. All films, regardless of the substrate used, were thermally treated following this procedure.

Cross sections of the as-deposited and annealed films obtained by cleavage were studied using a FEI Sirion 200 Scanning Electron Microscope. The individual layer and total thicknesses of the multilayers were determined by the Scanning Electron Microscope micrographs. The actual layer thicknesses are reported in Table 1 along with the nominal values.

The mechanical properties of the as-deposited and annealed films were measured using a Hysitron Triboscope with the nanoDMA™ attachment. Using this attachment the contact stiffness at various points during loading was recorded, which allowed the measurement of modulus and hardness as a function of penetration depth for a given indentation. A calibrated Berkovich tip was used for the indentation. All hardness values presented in this paper refer to values measured at contact depths that correspond to approximately 10% of the total film thickness in an effort to minimize any influence from the substrate on the measured values, while being deep enough to minimize any effects from surface roughness. Each sample was indented 5 times and 80 measurements per indent were collected. The values of hardness and modulus presented in this study are averages of the indentations.

The XPS spectra of the 100 nm/100 nm Mo/Pt films were obtained with an AXIS-165 manufactured by Kratos Analytical Inc. using an achromatic Mg Kα (1254 eV) X-ray radiation with a power of 210 W. The spectrometer was calibrated against both the Au $4f_{7/2}$ peak at 84.2 eV and the Ag $3d_{5/2}$ peak at 368.5 eV. Curve fitting of the XPS peaks was performed with the commercial CasaXPS software using Gaussian/Lorentzian line shape. The chemistry of the film was sampled by depth profiling. Ar^+ sputtering at 4 keV combined with XPS provided a way to analyze the first two layers of the multilayer sample under two conditions (as-deposited and annealed in air at 475 °C). In addition, XPS spectra of clean Mo and Pt were acquired for films prepared under the same sputtering conditions as the corresponding layers of the multilayer films. These spectra were used as reference.

Results and discussion

A typical micrograph from the surface of the as-deposited films can be seen in Fig. 1. The grains appear faceted and some voiding is present along the grain boundaries. The grain size ranged from 10 to 30 nm. The grain sizes for the as-deposited films were similar in all cases regardless of layer or total thickness. Representative cross sections of the as-deposited films can be seen in Figs. 2 and 3. The growth residual stress of the as-deposited 100 nm/100 nm Mo/Pt film was a compressive stress of 10.5 ± 0.7 MPa measured using bulge testing.

The hardness using nanoindentation, corresponding to a contact depth of approximately 10% of the film thickness, is presented in Table 2. It is apparent from these values that the thinner Pt layers provide higher strength composites, which is in accordance with results for other systems where the strength increases as the layer thickness decreases [1].

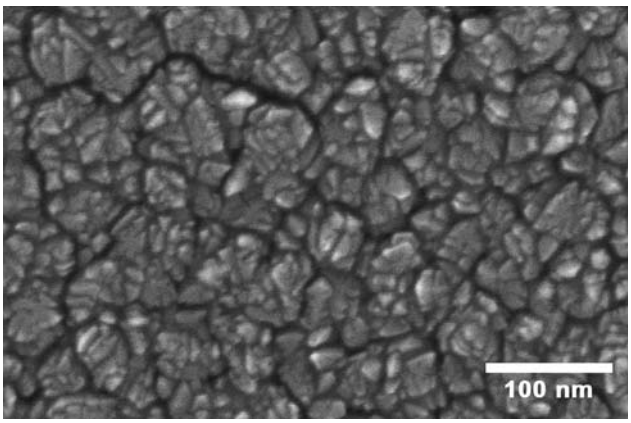

Fig. 1 Top view of the 35 nm/100 nm Mo/Pt film. The in-plane grain size of Pt is very small and some voiding can be seen along the grain boundaries

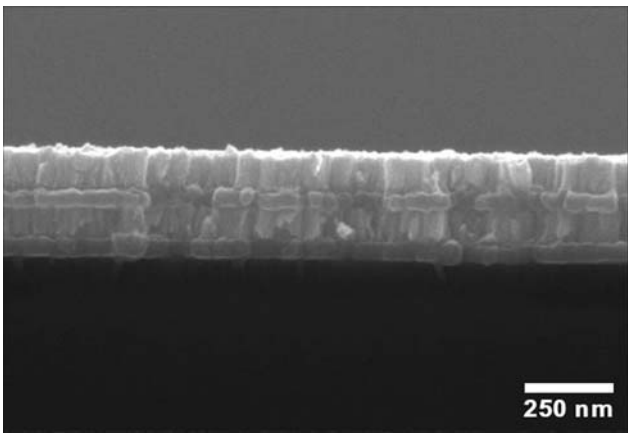

Fig. 2 Representative cross section of the 55 nm/100 nm Mo/Pt film. The lighter contrast layers with the distinct columnar structure of the grains are Pt layers

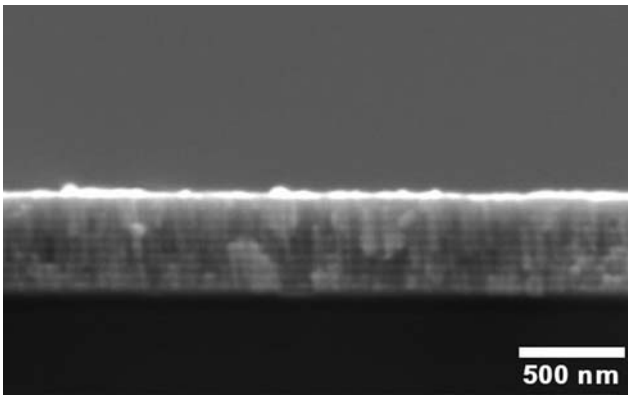

Fig. 3 Typical cross-sectional area of structure with 20 layers. The nominal layer thickness is 25 nm/30 nm (Mo/Pt)

The phase diagram of Mo–Pt shows that there is solubility over a significant range of compositions and exhibits a number of different intermetallics [14]. The study of annealed samples was necessary in order to determine whether the layered structure of the nanocomposites is maintained, if any intermetallics formed during the thermal processing, and how these microstructural changes affected the strength of the resulting films. For this reason the as-deposited films were annealed in air at 475 °C for 1 h.

After annealing the residual stress of the 100 nm/100 nm film became tensile and a value of 38.4 ± 1.6 MPa was measured using bulge testing. The relatively small difference in the values of the net residual stress for the same film before and after annealing indicates that the net stress of the multilayers may not be an important factor in the overall behavior of the films with the stresses in the individual layers possibly playing a more important part.

The modulus and hardness of the annealed samples as a function of contact depth were again measured using nanoindentation and the corresponding values of hardness are presented in Table 2. In all cases the strength of the annealed films was lower than what was determined for the as-deposited films; with the decrease being more significant for the thinner Pt layers. Despite this decrease the hardness of all annealed films was still higher than that of 200 nm Pt films annealed at the same temperature (2.63 GPa). Comparison between the hardness versus contact depth for the as-deposited and annealed case can be seen for two of the samples in Fig. 4. In order to explain the strength loss and the difference in behavior between thinner and thicker layers the microstructure of the annealed films was studied using the SEM.

In Fig. 5a and b the top view and cross section of the annealed 55 nm/100 nm Mo/Pt film are shown. After the heat treatment the slightly voided boundaries open significantly, forming cracks along the Pt grain boundaries. The in plane grain size is larger than what was observed for the as-deposited films, ranging from 20 to 50 nm. This grain coarsening can be responsible for the observed decrease in strength. Comparing the cross section of the as-deposited sample (Fig. 2) to the one after annealing (Fig. 5b) it is apparent that a significant change in the microstructure has occurred. Although after the heat treatment the layering of the composite was maintained, the thickness of all the Mo layers has significantly increased. This increase in the thickness of the Mo layers was typical for all the structures with the thicker Pt layers; namely samples 4, 5, and 6. A possible explanation for the increase in thickness is the oxidation of Mo. Mo oxides have lower densities than Mo, and hence a significant increase in volume is observed during oxidation [15]. This volume expansion likely causes

Table 2 Comparison of hardness values for all films before and after annealing

Nominal layered film (Mo/Pt)	H (GPa)	H (GPa) annealed	% decrease in strength after annealing
20 nm/20 nm	6.62 ± 0.26	4.17 ± 0.19	37
25 nm/30 nm	6.29 ± 0.29	3.71 ± 0.75	41
60 nm/35 nm	5.85 ± 0.52	4.37 ± 0.71	25
35 nm/100 nm	3.67 ± 0.41	2.87 ± 0.49	22
55 nm/100 nm	3.8 ± 0.45	3.36 ± 0.52	12
100 nm/100 nm	4.29 ± 0.30	3.32 ± 0.40	23
200 nm Pt (single layer)	–	2.63 ± 0.45	–

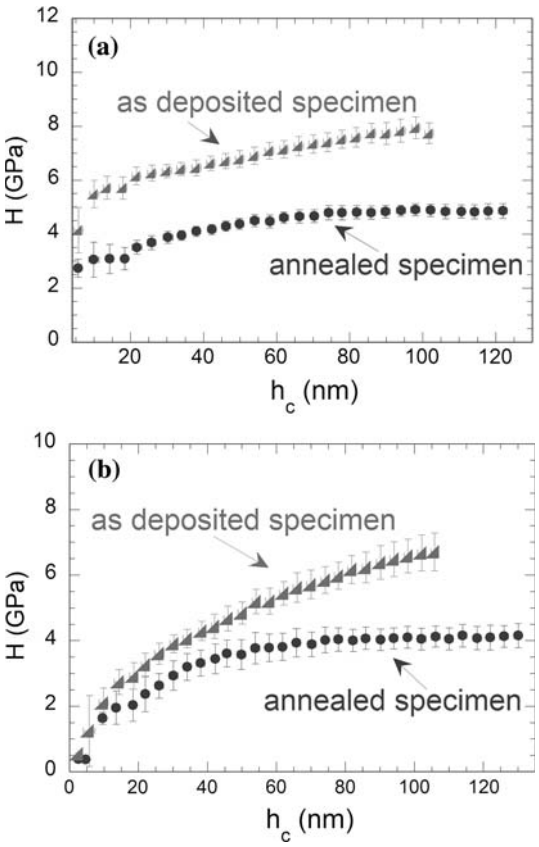

Fig. 4 Representative curves of hardness versus contact depth for as-deposited and annealed samples. In both **a** (20 nm/20 nm Mo/Pt film) and **b** (100 nm/100 nm Mo/Pt film) the hardness values for the annealed composites are lower than the corresponding values in the as-deposited case

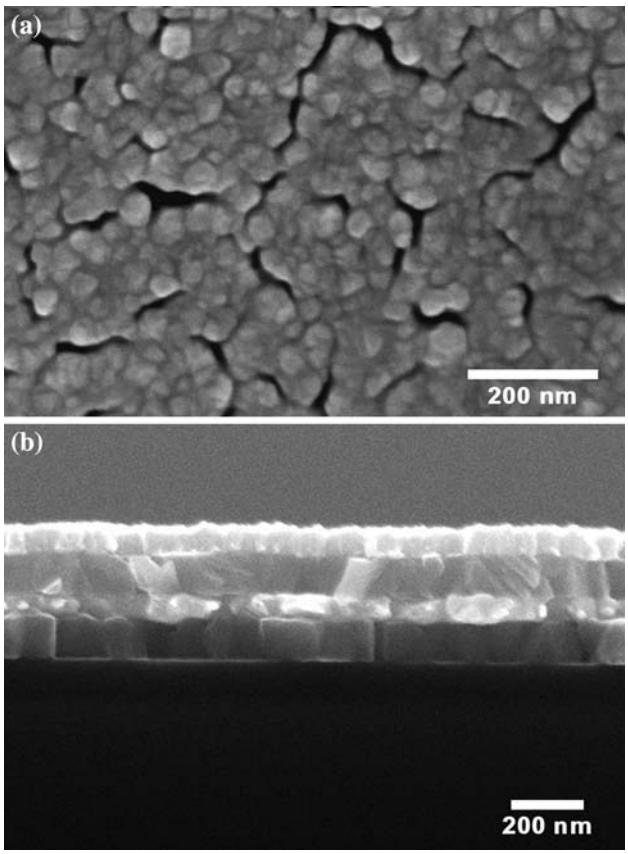

Fig. 5 **a** Typical top view of the film surface for annealed samples with thicker layers. Cracking along the grain boundaries is present. **b** Cross section of the 55 nm/100 nm Mo/Pt film after annealing at 475 °C for an hour. The thickness of the Mo layers (darker contrast) considerably increased during annealing compared to the initial thickness (Fig. 2)

the observed cracking along the grain boundaries. Although in these multilayered structure Pt as the top layer is directly in contact with air, diffusion of oxygen can occur along the Pt grain boundaries causing oxidation of the underlying Mo layers. It is probable that oxygen diffusion is further enhanced by the crack formation. X-ray Photoelectron Spectroscopy and X-ray Diffraction were used to verify that oxidation is responsible for the apparent changes in microstructure.

Figure 6 shows the Pt 4f and Mo 3d spectra. Both reference spectra of Pt 4f and Mo 3d and spectra obtained at sputtering times of about 3400 and 11400 s from the annealed 100 nm/100 nm Mo/Pt film are shown for comparison. The Pt 4f spectrum (Fig. 6a) acquired after 3400 s of Ar sputtering (Pt layer) shows no peak shift. Pt appears in its elemental metallic form, Pt^0, which indicates that no Pt/Mo intermetallics formed during the annealing process. Figure 6b shows XPS spectra of Mo 3d from the reference Mo film, along with spectra from the as-deposited and the annealed 100 nm/100 nm Mo/Pt multilayer after 11400 s of Ar sputtering. The spectra for the reference film and the as-deposited nanocomposite film exhibit similar Mo species. The main peak at a binding energy of (BE) = 228.1 ± 0.1 eV is assigned to elemental Mo^0, in good agreement with literature values [16, 17]. A weak peak at BE = 229.4 eV is assigned to Mo^{4+} due to oxygen present in the film. This peak is associated with MoO_2. The XPS spectrum of Mo for the annealed sample after 11400 s of Ar sputtering displays at least two Mo oxide species. Deconvolution of the 3d doublet reveals the existence of Mo dioxide (Mo^{4+}) and trioxide species (Mo^{6+}). No pure Mo peak is identified in the annealed sample. An XPS survey of the sample well within the Mo layer confirms the presence of a large amount of oxygen (~52 at.%) in agreement with the findings of the peak deconvolution. The values for the binding energies and the oxides associated with each peak are presented in Table 3, and show that annealing the multilayered film led to the complete oxidation of Mo to form MoO_2, $Mo_x(OH)_y$, and MoO_3 while no Mo–Pt intermetallics formed. Using the amount of hydroxide obtained from the O 1s peak (not shown) the

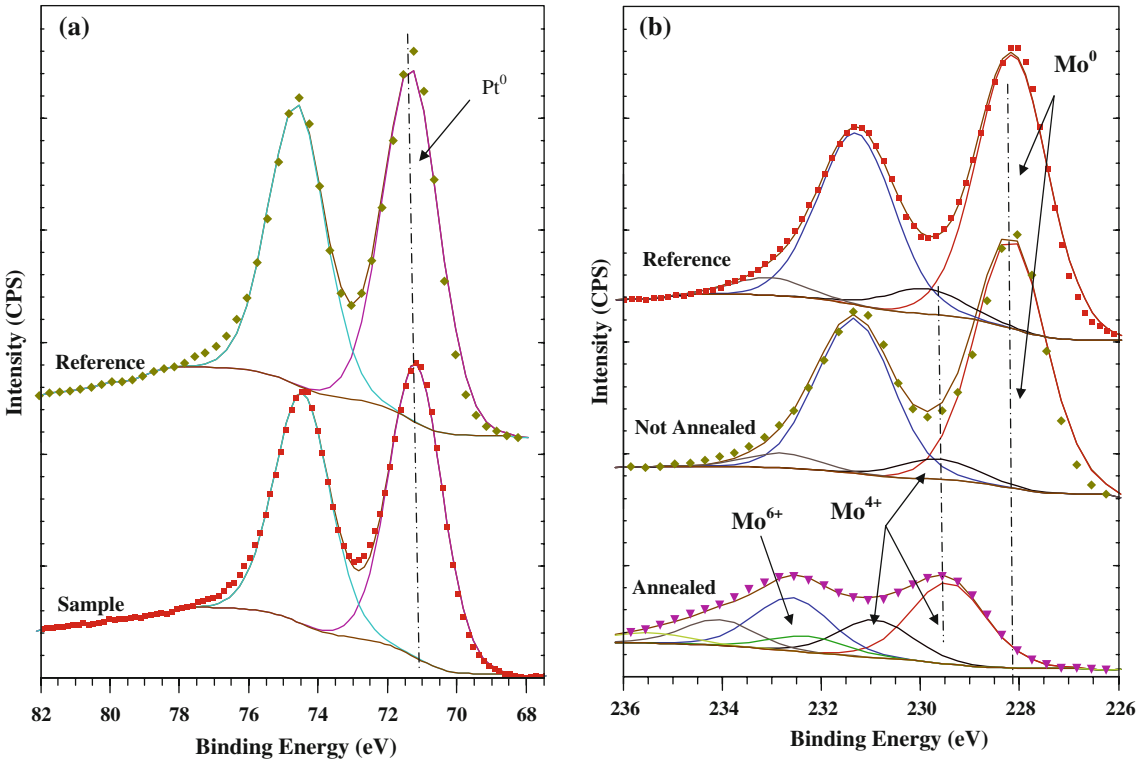

Fig. 6 Spectra obtained from XPS of the 100 nm/100 nm Mo/Pt film. **a** Pt 4f XPS spectra. No shift was observed between the reference (top spectrum) and the spectrum obtained after about 3400 s of Ar^+ sputtering of the annealed film (Pt layer). **b** Mo 3d spectrum from the reference film and peaks obtained before and after annealing of the composite at about 11400 s of Ar^+ sputtering (Mo layer)

Table 3 Binding energies and most probable oxidation states of Mo in annealed Pt/Mo multilayers

Peak	Binding energy of the $3d_{5/2}$ peak (eV)	Oxidation state of Mo
1	228.1	Mo^0 [16, 17]
2	229.4	Mo^{+4} [17]
3	231.0	Mo^{+4} [18] due to OH
4	232.3	Mo^{+6} [18]

value of x and y were determined to be close to 1:1, respectively. Any intermetallics which formed during annealing would have resulted in a BE shift of 0.3–0.9 eV of the metallic main peak (Mo^0), as shown by Jaksic et al. [19] in their work on Mo–Pt alloying. No such energy shift was measured for our sample.

Since XPS was only used to probe the first Mo layer (second layer in the stacking sequence) and identify the different oxidation states of Mo, X-ray diffraction was further utilized to verify that complete oxidation of all the Mo layers has occurred. X-ray diffraction patterns collected from the annealed 100 nm/100 nm Mo/Pt film deposited on a glass substrate can be seen in Fig. 7. In addition to peaks corresponding to Pt, Mo oxide peaks were clearly identified, whereas no peaks corresponding to pure Mo were present. These results combined with the apparent increase in the thickness of all the Mo layers in the annealed structures suggest that complete oxidation of the Mo layers has occurred upon annealing.

Annealing structures with thinner Pt layers resulted in somewhat different microstructures than the ones described for those with the thickest Pt layers (100 nm).Top view and cross-sectional micrographs for the case of the 25 nm/30 nm Mo/Pt film are shown in Fig. 8. The micrographs presented here are typical for all structures with Pt layers thinner than 35 nm layers (samples 1–3). As was previously observed for structures with thicker layers (Fig. 5b) the thickness of all the Mo layers has significantly increased after annealing (Fig. 8b) compared to the as-deposited case (Fig. 3). This behavior is again indicative of oxidation during the thermal treatment. However, in this case the layered structure was not maintained, with Pt appearing in the form of isolated islands rather than layers. The loss of the continuous interface is likely responsible for the significant decrease in strength recorded for all structures with thinner layers and presented in Table 2.

The top view of the annealed sample (Fig. 8a) also demonstrates a feature that indicates the importance of

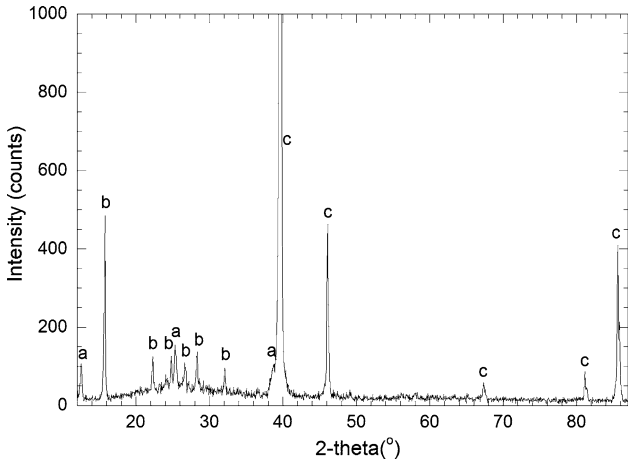

Fig. 7 X-ray diffraction pattern for the 100 nm/100 nm Mo/Pt film annealed at 475 °C for 1 h. *a* denotes the peaks assigned to MoO_3 (pdf #005-0508), *b* corresponds to the $Mo_{17}O_{47}$ peaks (pdf #013-0345), and *c* marks the positions of the Pt diffraction peaks (pdf #004-0802)

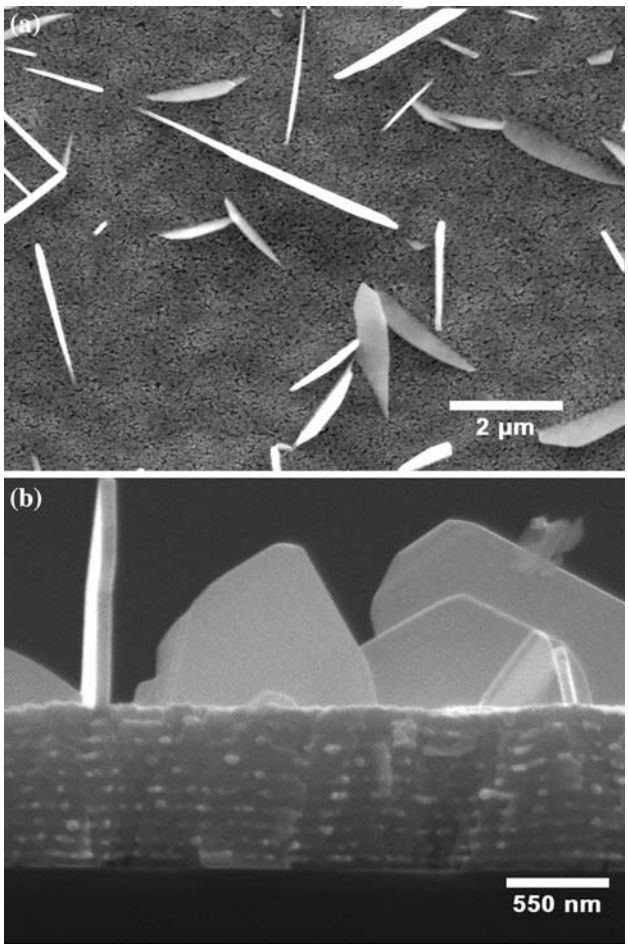

Fig. 8 **a** Top view of the 25 nm/30 nm Mo/Pt film after it was annealed at 475 °C for 1 h. In addition to significant cracking other features are present on the surface, identified as MoO_3 platelets. **b** Cross section of the 25 nm/30 nm Mo/Pt annealed film where the disruption of the layered structure is apparent with Pt appearing in the form of islands (light contrast areas of the multilayer)

oxidation in this system. In addition to cracking that was observed for the 4 layer films, white faceted platelets are also present on the sample surface. These faceted platelets have similar appearance to MoO_3 platelets that form during oxidation of Mo. A study of the oxidation of Mo silicides in air [20] showed that at 600 °C the sample surface was covered by white powder and XRD identified MoO_3 as the primary phase. In their work, annealing at 800 °C caused complete volatilization of the MoO_3 phase which was deposited on areas of lower temperature in the reaction chamber in the form of spikes. The volatile nature of molybdenum trioxide has been utilized in the synthesis of MoO_3 whiskers by oxidation of Mo in an oxygen atmosphere where the temperature in the furnace reached 900 °C [21]. Although in both these papers volatilization seems to occur at higher temperatures than the one used here, in Ref. [22] partial vaporization of the forming oxide was reported for temperatures between 550 and 700 °C. These observations in literature over a wide range of oxygen pressures, combined with the fact that the formation of molybdenum trioxide is an exothermic reaction that releases significant amounts of heat [20, 22] make the volatilization of MoO_3 a mechanism that could operate even at the moderate annealing temperature of 475 °C used in this study. This could also explain how oxide platelets appeared on the surface of the film despite the fact that Pt is the layer in direct contact with air. Diffusion of oxygen along the Pt grain boundaries caused the formation of various Mo oxides and a significant increase in volume. The heat released by the oxidation process locally increased the temperature, allowing the vaporization of molybdenum trioxide. The cracking that occurred along the grain boundaries in the case of thin Pt layers along with the loss of the continuous interface between the two metals exposed the Mo layers and allowed MoO_3 vapors to escape from the film. Condensation of the oxide vapors is expected on areas of lower temperatures (which can either be the surface of the sample or other areas inside the furnace). If this is the case, material loss from the film would be observed. This material loss was indeed observed for the 25 nm/30 nm Mo/Pt film deposited on the glass substrate. Before the thermal treatment at 475 °C the surface of the film was reflective and no cracks could be seen macroscopically. However, after annealing of the film macroscopic cracks which exposed the glass substrate were present indicative of significant material loss.

X-ray diffraction of the annealed 25 nm/30 nm Mo/Pt film that was deposited on the glass substrate, shown in Fig. 9, confirmed the presence of Molybdenum oxides and

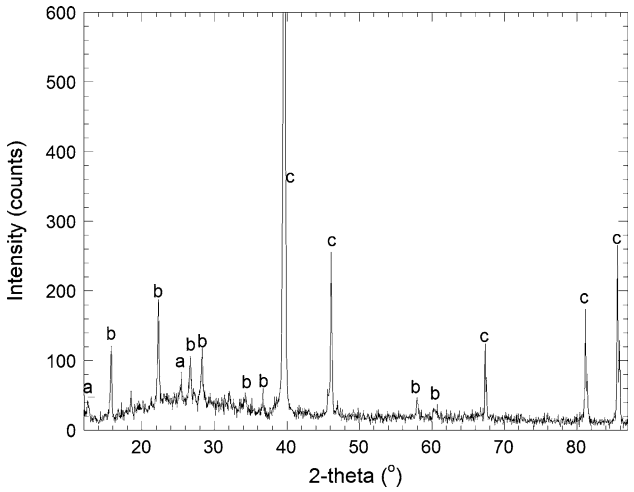

Fig. 9 X-ray diffraction pattern for the 25 nm/30 nm Mo/Pt film annealed at 475 °C for 1 h. *a* denotes the peaks assigned to MoO_3 (pdf #005-0508), *b* corresponds to the $Mo_{17}O_{47}$ peaks (pdf #013-0345), and *c* marks the positions of the Pt diffraction peaks (pdf #004-0802)

the absence of pure Mo in the sample. Although peaks corresponding to MoO_3 are still present; they are not as well defined as the same peaks in the X-ray diffraction of the annealed samples with thicker Pt layers that did not undergo this platelet growth. This observation is in accordance with oxide volatilization during the annealing process once the Pt layer has lost continuity. Again the findings of the X-ray diffraction, combined with the increase in the thickness of the Mo layers in the structures, suggest complete oxidation of all the Mo layers. The only difference from structures with thicker Pt layers is that here spheroidization of the Pt layers occurred which allowed partial volatilization of the forming oxide with subsequent growth of MoO_3 platelets on the surface.

From these findings it is apparent that the annealing of the composites causes a change in microstructure which results in lower strength. The difference in the magnitude of the strength decrease for structures with thinner and thicker Pt layers indicates that different length scales are responsible for the observed strengthening of the as-deposited films. Strengthening of polycrystalline multilayers relies on two length scales of interest; layer thickness and grain size [23]. When the in-plane grain size is much smaller than the layer thickness both grains and interfaces play a role in the observed behavior. The hardness in that case will show a Hall–Petch type of dependency and will be associated with pile ups at the grain boundaries and the interfaces between the two layers. In Ref. [7] it is reported that for Cu composites with layer thicknesses larger than 50 nm the Hall–Petch model can explain the hardening behavior with both grain boundaries and interfaces acting as barriers to dislocation motion. However, as the layer thickness becomes smaller the interfaces will dominate the mechanical behavior by confining the dislocation motion within the soft layers of the nanostructure. These mechanisms correlate well with the observed mechanical behavior of the Mo/Pt multilayers. For the composites with a Pt layer of 100 nm, both grain size and interfaces determine the overall strength. After annealing the interface is maintained, despite apparent changes in layer thickness due to oxidation, and the observed decrease in strength can be justified by grain coarsening that occurs during annealing. However, for the multilayers with the smaller Pt thicknesses the interfaces dominate the strengthening behavior. The loss of the continuous interface between the Mo and the Pt layer is responsible for the large decreases in strength that cannot be justified by grain coarsening alone.

Summary

Annealing of Mo/Pt multilayer films in air at 475 °C causes changes in the films microstructure, regardless of layer thickness. These changes are more significant when the Pt layers are thin, 20–35 nm in this study, where disruption of the layering occurred along with destructive oxidation of Mo, which involved vaporization of the forming oxide. For the 100 nm Pt thicknesses no spheroidization was observed and although again complete oxidation of all the Mo layers occurred, the Pt layers protected Mo from destructive oxidation. A novel growth mode in the oxidizing layers was demonstrated; despite the increase in the total film thickness the layered structure of the films was maintained indicative of a uniform oxidation process. These differences in microstructure between thinner and thicker layers are reflected in the strength loss after annealing of the various films. For the thicker Pt layers a significant amount of the as-deposited strength is maintained, with the softening likely due to an increase of the in-plane grain size from 10–30 nm to 20–50 nm. Films with thinner Pt layers exhibit a larger decrease in strength. The loss of the continuous interface between the Mo and the Pt layers, followed by the substantial oxidation and evaporation of the solid MoO_3, is proposed as being responsible for the large losses in strength. These results show that although thinner layers lead to stronger films at room temperature, thicker layers with the subsequent sacrifice in initial strength should be used for high temperature applications in order to maintain a substantial fraction of the strength and integrity of the film, as they are approximately 20% harder than pure Pt films after the same annealing treatment.

Acknowledgement This work was supported in part by the US Department of Energy under Grant number DE-FG02-07ER4635.

References

1. Misra A, Hirth JP, Kung H (2002) Philos Mag A 82:2935
2. Was GS, Foecke T (1996) Thin Solid Films 286:1
3. Misra A, Kung H (2001) Adv Eng Mater 3:217
4. Misra A, Hirth JP, Hoagland RG (2005) Acta Mater 53:4817
5. Lee HJ, Kwon KW, Ryu C, Sinclair R (1999) Acta Mater 47:3965
6. Misra A, Hoagland RG (2005) J Mater Res 20:2046
7. Misra A, Verdier M, Lu YC, Kung H, Mitchell TE, Nastasi M, Embury JD (1998) Scripta Mater 39:555
8. McKeown J, Misra A, Kung H, Hoagland RG, Nastasi M (2002) Scripta Mater 46:593
9. Huang H, Spaepen F (2000) Acta Mater 48:3261
10. Eakins LMR, Olson BW, Richards CD, Richards RF, Bahr DF (2003) Thin Solid Films 441:180
11. Morris DJ, Bahr DF, Anderson MJ (2008) Sens Actuators A 141:262
12. Bonnotte E, Delobelle P, Bornier L, Trolard B, Tribillon G (1997) J Mater Res 12:2234
13. Vlassak JJ, Nix WD (1992) J Mater Res 7:3242
14. Massalski TB (1986) Binary alloy phase diagrams. American Society for Metals, Metals Park, OH
15. Underwood JH, Gullikson EM, Nguyen K (1993) Appl Opt 32:6985
16. Werfel F, Minni E (1983) J Phys C: Solid State Phys 16:6091
17. Barr TL (1978) J Phys Chem 82:1801
18. Brox B, Olefjord L (1988) Surf Interface Anal 13:3
19. Jaksic JM, Vracar Lj, Neophytides SG, Zafeiratos S, Papakonstantinou G, Krstajic NV, Jaksic MM (2005) Surf Sci 598:156
20. Natesan K, Deevi SC (2000) Intermetallics 8:1147
21. Geng DY, Zhang ZD, Zhang M, Li D, Song XP, Hu KY (2004) Scripta Mater 50:983
22. Gulbransen EA, Andrew KF, Brassart FA (1963) J Electrochem Soc 110:952
23. Misra A, Verdier M, Kung H, Embury JD, Hirth JP (1999) Scripta Mater 41:973